Li_3BO_3 and Li_3BN_2: Computational Study of Structural and Electrolyte Properties of Pure and Doped Crystals

Yan Li[1], Zachary D. Hood[2], Natalie A. W. Holzwarth[1]

[1]Department of Physics, Wake Forest University, Winston-Salem, NC 27109, USA

[2]Applied Materials Division, Argonne National Laboratory, Argonne, IL 60439, USA

APS March Meeting 2021

Session E61: Energy Research -- Energy Storage I

Outlines

Inequiv. Li B O N

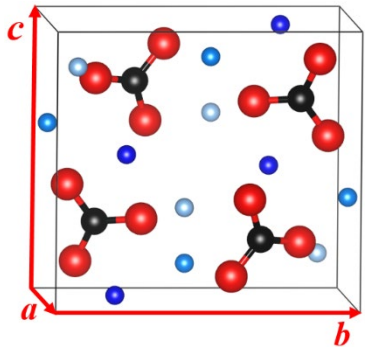

Li_3BO_3
Monoclinic $P2_1/c$ (#14)[1]
4 formula units / unit cell

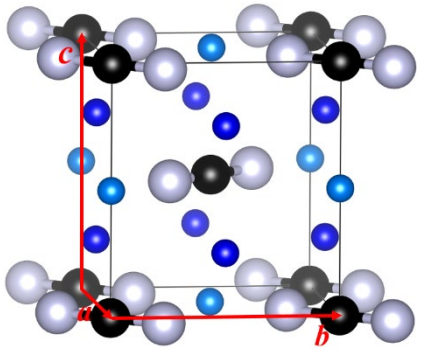

α-Li_3BN_2
Tetragonal $P4_2/mnm$ (#136)[2]
2 formula units / unit cell

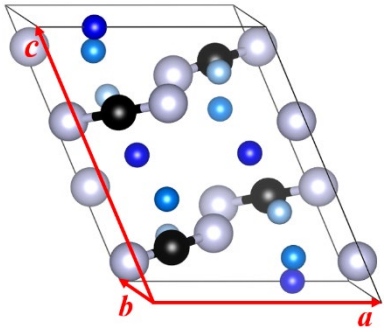

β-Li_3BN_2
Monoclinic $P2_1/c$ (#14)[2]
4 formula units / unit cell

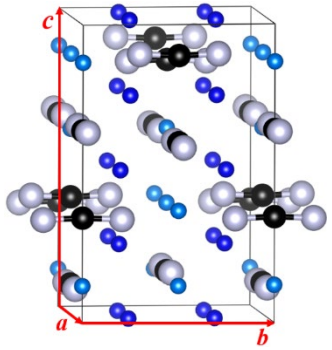

γ-Li_3BN_2
Tetragonal $I4_1/amd$ (#141)[3]
8 formula units / unit cell

Focuses of this presentation:

- ❑ Structure correction for α-Li_3BN_2
- ❑ Electrolyte properties of pure and doped Li_3BO_3 and β-Li_3BN_2 crystals
- ❑ Stability analysis of the ideal interfaces of pure Li_3BO_3 and β-Li_3BN_2 with Li metal anode

[1]Stewner, *Acta Crystallogr. section B.* **27**, 904 (1971)
[2]Yamane et al., *J. Solid State Chem.* **71**, 1-11 (1987)
[3]Pinkerton and Herbst, *J. Appl. Phys.* **99**, 113523 (2016)

Summary of computational methods

- Density Functional Theory (DFT) and Density Functional Perturbation Theory (DFPT) with the modified Perdew-Burke-Ernzerhof generalized gradient approximation[1] **(PBEsol GGA)**
- The projector augmented wave (PAW) formalism using ABINIT (https://www.abinit.org) & QUANTUM ESPRESSO (http://www.quantum-espresso.org)
- Datasets generated by ATOMPAW code available at http://pwpaw.wfu.edu
- Visualization software: XCrySDen, VESTA
- Space-group analysis: FINDSYM
- X-ray diffraction: Mercury

[1]Perdew et al., *Phys. Rev. L.* **100**, 136406 (2008)

Corrected α phase of Li_3BN_2

Li(4d)
Li(2b)

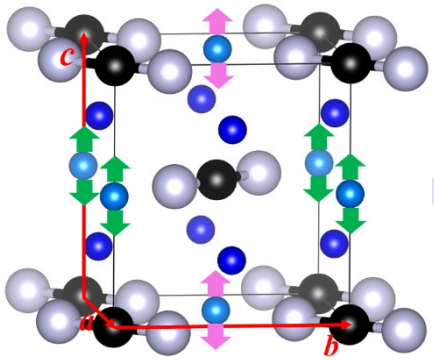

Modes #1&2 at M (0.5, 0.5, 0)

$$\mathbf{a_s} = a_c\hat{\mathbf{x}} + b_c\hat{\mathbf{y}}$$
$$\mathbf{b_s} = a_c\hat{\mathbf{x}} - b_c\hat{\mathbf{y}}$$
$$\mathbf{c_s} = c_c\hat{\mathbf{z}}$$

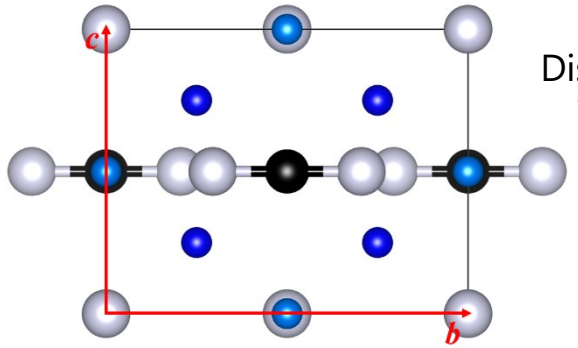

Super tetragonal $P4_2/mnm$

Distort b-type Li ions along c

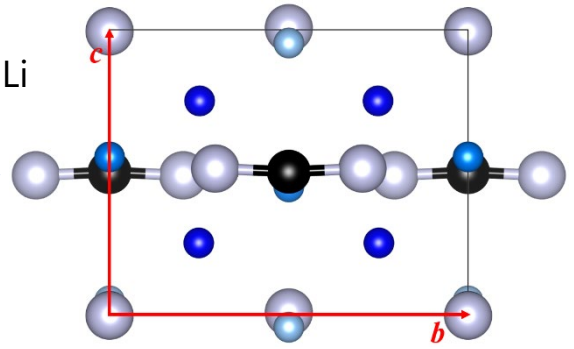

Orthorhombic Pmmn

Li(8g)
Li(2a)
Li(2b)

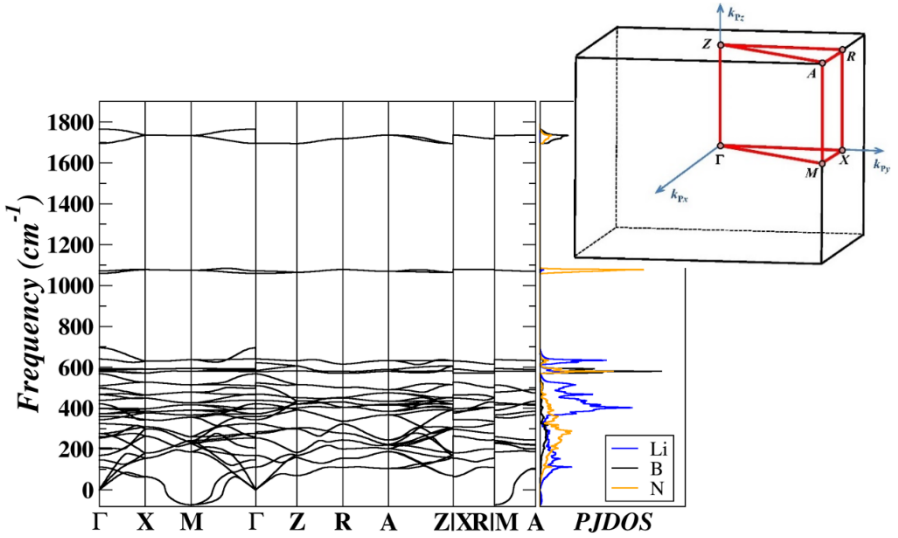

Reported α-Li_3BN_2 in the $P4_2/mnm$ structure

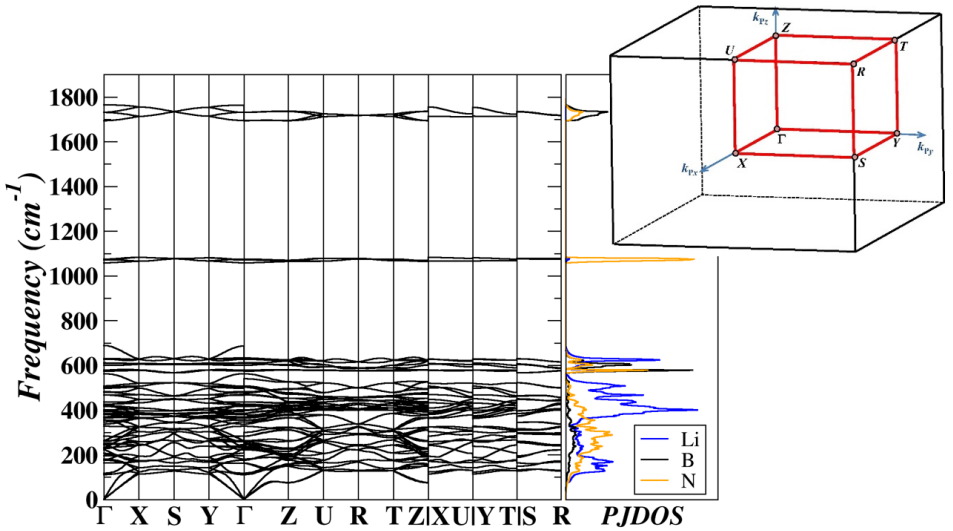

New α-Li_3BN_2 in the Pmmn structure

Brillouin zone diagrams: Hinuma et al., *Comp. Mat. Sci.* **128**, 140-184 (2017)

Harmonic vs. Quasi-harmonic

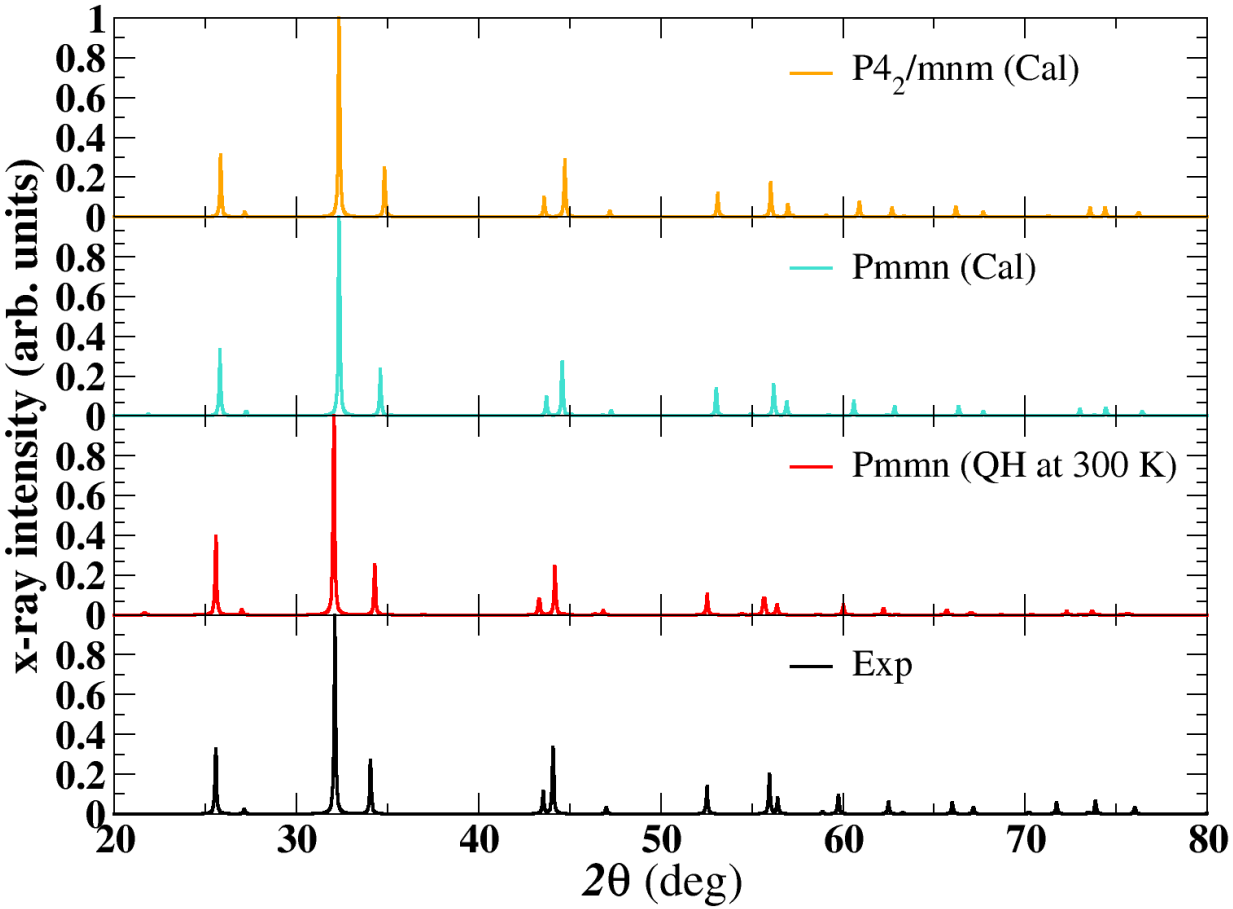

Comparison of simulated and experimental x-ray diffraction (λ = 1.54056 A°) patterns.

Exp: Yamane et al., *J. Solid State Chem.* **71**, 1-11 (1987)

Defect models for monoclinic Li_3BO_3 and β-Li_3BN_2

Inequiv. host Li interstitial Li

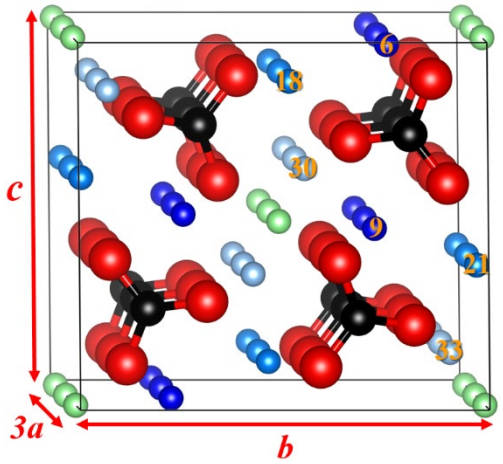

3x1x1 supercell of Li_3BO_3 ($P2_1/c$)

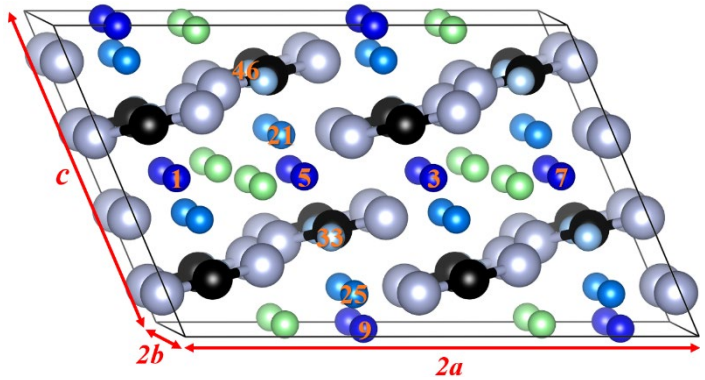

2x2x1 supercell of β-Li_3BN_2 ($P2_1/c$)

Metastable interstitial defects (green balls):

- Li_3BO_3: Wyckoff sites *2b* with coordinates (0.5, 0.5, 0.5); E_f = 1.25 eV
- Li_3BN_2: Wyckoff sites *4e* with coordinates (0.560, 0.279, 0.978); E_f = 1.23 eV

Models of Li-deficient structures:

- Pure crystal with an ideal Li vacancy created by removing a Li ion and compensating with a uniform charge of the opposite sign -- **I-vac**
- F-doped crystal with the stoichiometry of $Li_{3-x}BO_{3-x}F_x$ (x = 1/12) -- **F-doped**
- C-doped crystal with the stoichiometry of $Li_{3-x}B_{1-x}C_xN_2$ (x = 1/16) -- **C-doped**

Stability analysis:

- $\mathrm{Li_{3-x}BO_{3-x}F_x} \rightarrow (1-2x)\ \mathrm{Li_3BO_3} + 2x\ \mathrm{Li_2O} + x\ \mathrm{B_2O_3} + x\ \mathrm{LiF} - 0.06\ \mathrm{eV}$
- $\mathrm{Li_{3-x}B_{1-x}C_xN_2} \rightarrow (1-x)\ \mathrm{Li_3BN_2} + x\ \mathrm{Li_2CN_2} + 0.05\ \mathrm{eV}$

Li ion vacancy migration analysis via Elastic Band Method[1,2]

Inequiv. Li

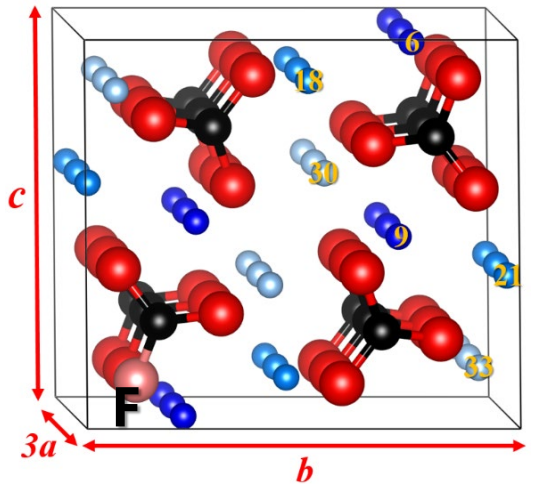

Li_3BO_3

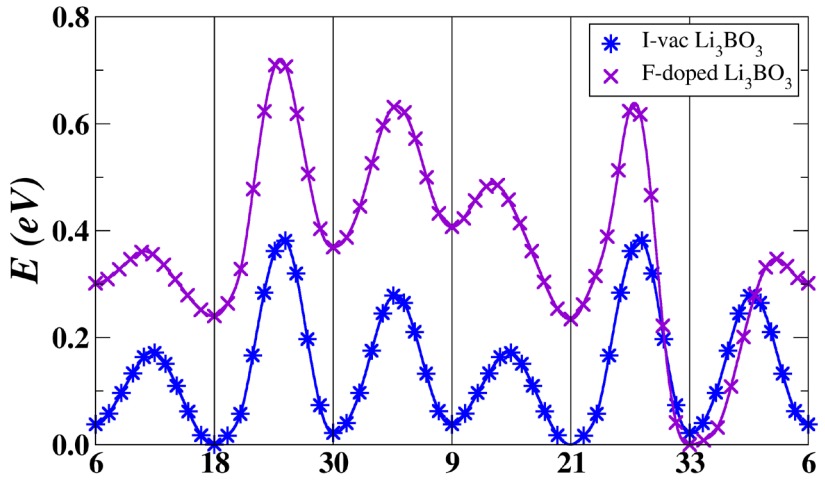

$$\epsilon_{\min} \leq E_a^{\mathrm{NEB}} \leq \epsilon_{\max}$$

For I-vac and doped crystals:

$$\epsilon_{\min} = E_m^{\mathrm{NEB}} = \max\left(\Delta E_m + E_d^0\right)$$

For perfect crystals:

$$\epsilon_{\max} = E_m^{\mathrm{NEB}} + \frac{1}{2}E_f$$

Recall E_f = 1.25 eV for Li_3BO_3 and 1.23 eV for Li_3BN_2.

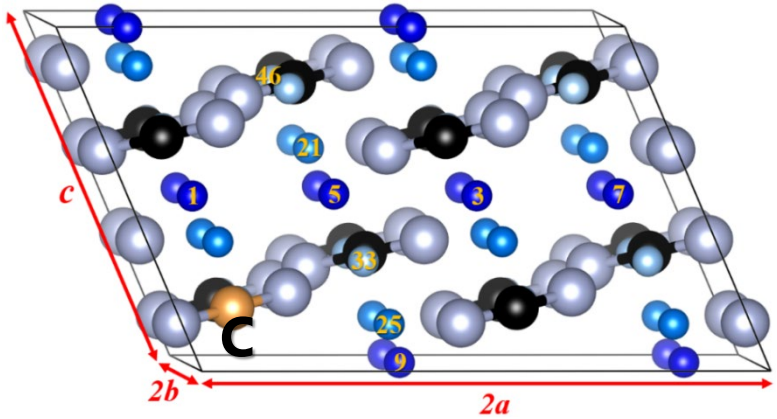

Li_3BN_2

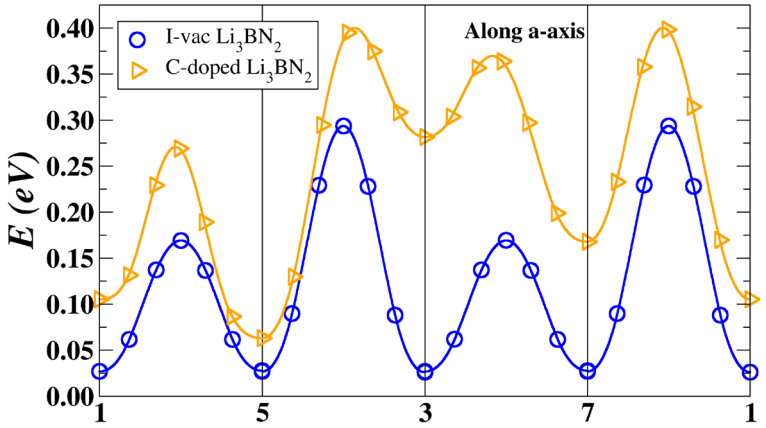

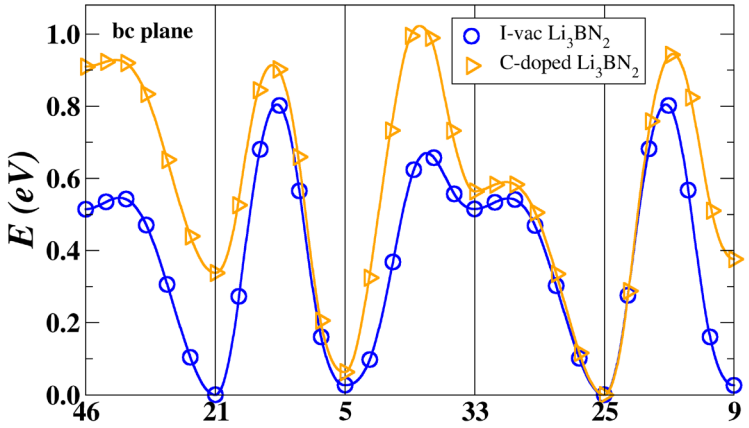

[1]Jónsson et al., *in Classical and Quantum Dynamics in Condensed Phase Simulations*, edited by B. J. Berne, G. Ciccotti, and D. F. Coker (World Scientific, Singapore, 1998)

[2]Henkelman et al., *J. Chem. Phys.* **113**, 9901-9904 (2000)

Molecular dynamics simulations

NVE ensemble

$$\langle T \rangle = \frac{2}{3(N_{\text{atom}} - 1)k_B} \frac{1}{(t_{\max} - t_{\text{eq}})} \int_{t_{eq}}^{t_{\max}} E_{\text{kin}}^{\text{ion}}(t')\,dt'$$

$$\text{MSD}(t,T) \equiv \frac{1}{N_{\text{Li}}} \left\langle \sum_{i=1}^{N_{\text{Li}}} |\mathbf{R}_i(t) - \mathbf{R}_i(0)|^2 \right\rangle$$

$$D_{tr}(T) = \frac{1}{6} \lim_{t\to\infty} \frac{1}{(t - t_{eq})} \text{MSD}(t - t_{eq}, T)$$

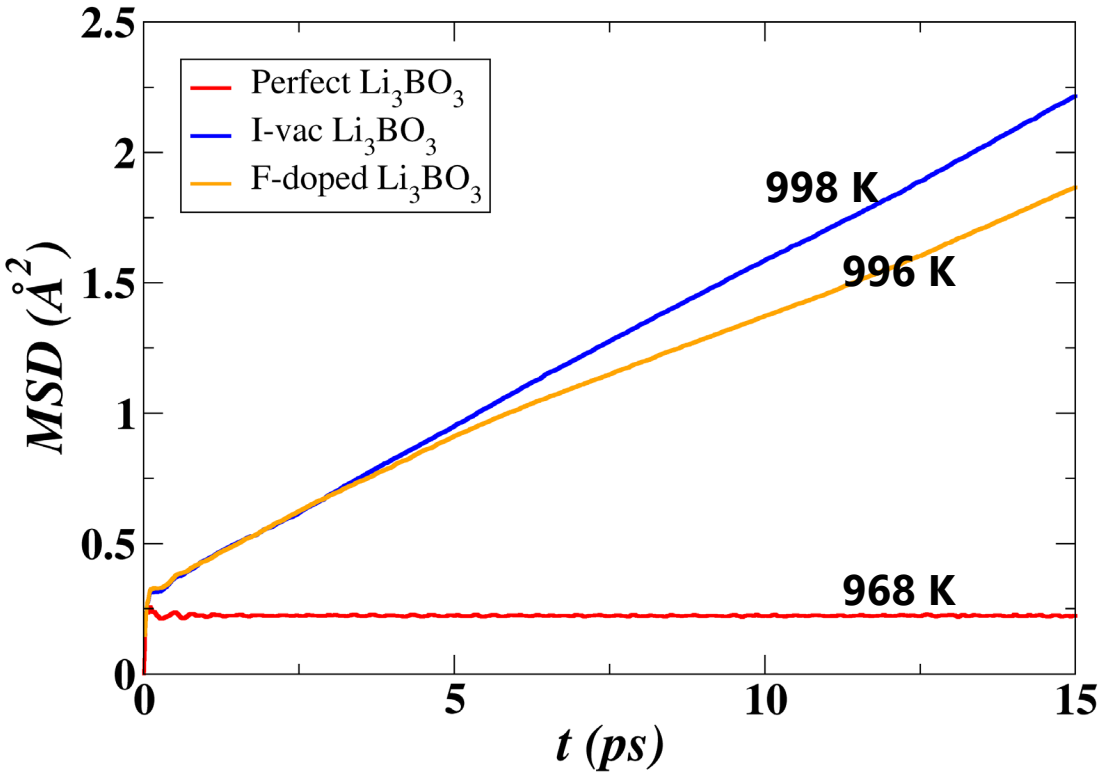

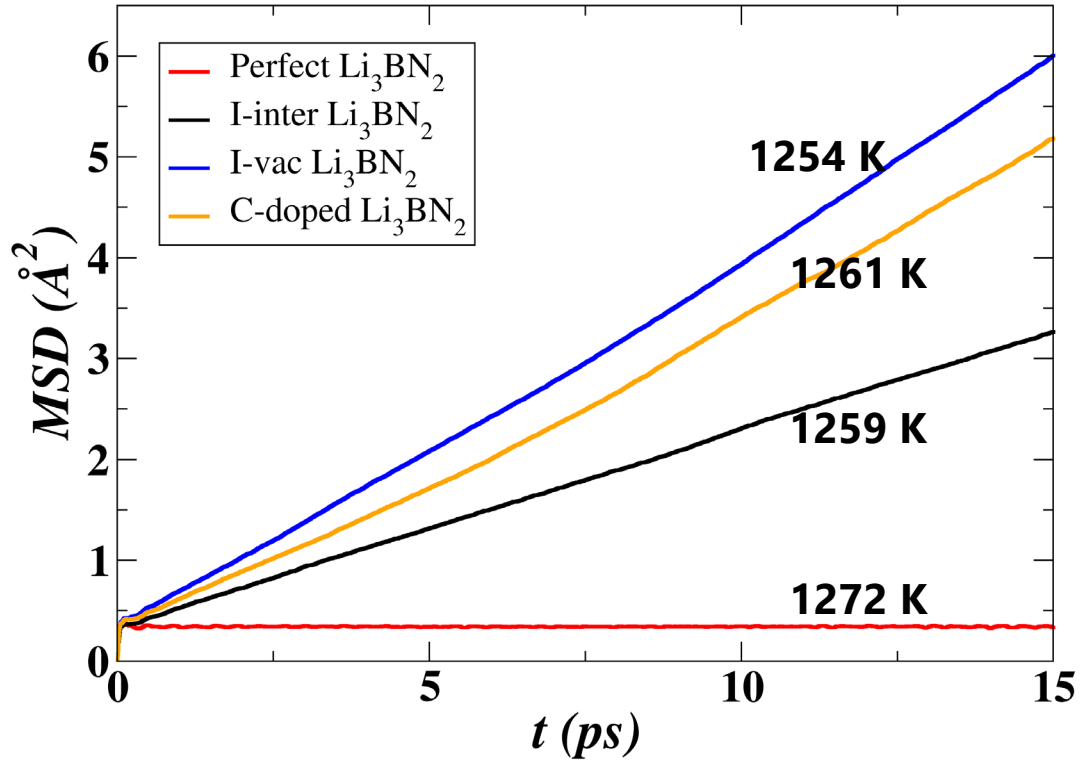

Ionic conductivities

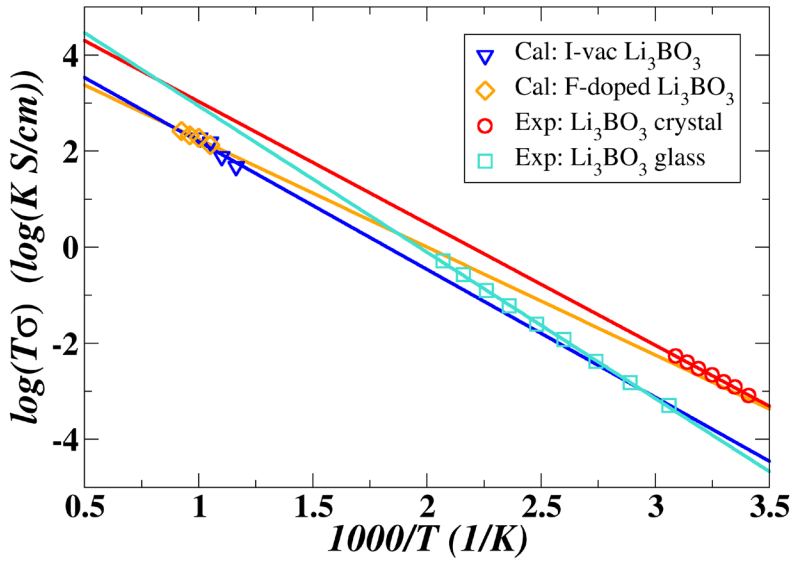

Li_3BO_3

Materials	Analysis	E_a	σ (T = 300 K)
I-vac Li_3BO_3	MD	0.53	3.2 x 10^{-7}
	NEB	0.38	--
F-doped Li_3BO_3	MD	0.45	3.4 x 10^{-6}
	NEB	0.72	--
Polycrystalline Li_3BO_3	Exp[1]	0.51	2.0 x 10−6
Glassy Li_3BO_3	Exp[2]	0.60	3.4 x 10−7

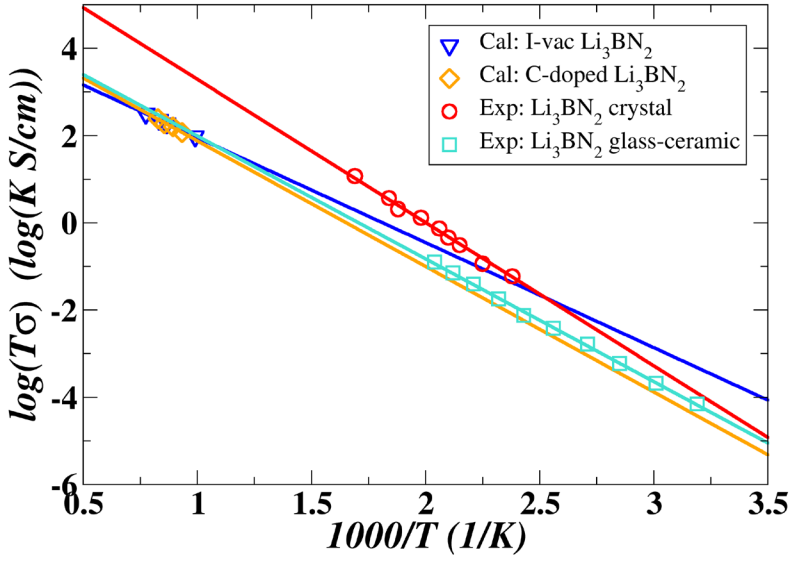

Li_3BN_2

Materials	Analysis	E_a	σ (T = 300 K)
I-vac Li_3BN_2	MD	0.48	7.2 x 10^{-7}
	NEB	0.30 (**a**)/0.81 (**bc**)	--
C-doped Li_3BN_2	MD	0.57	4.8 x 10^{-8}
	NEB	0.40 (**a**)/1.02 (**bc**)	--
Polycrystalline Li_3BN_2	Exp[2]	0.66	1.4 x 10−7
Glassy-ceramic Li_3BN_2	Exp[3]	0.56	1.1 x 10−7

Exp[1]: Ohta *et al.*, *J. of Power Sources* **238**, 53 (2013)
Exp[2]: Yamane *et al.*, *J. Solid State Chem.* **71**, 1 (1987)
Exp[3]: Shigeno *et al.*, *Solid State Ion.* **339**, 114985 (2019)

$$\sigma(T) = \rho q^2 \frac{D_{tr}(T)}{k_B T H_r} \quad \text{with} \quad D_{tr}(T) = D_0 e^{-E_a^{\mathrm{MD}}/k_B T}$$

Interfaces with Li metal anode

Li B O N

Predicted reactions:

$$\Delta F = \sum_i F_i^P - \sum_j F_j^R$$

Reaction: R → P	ΔU_{SL}	ΔF_{vib}	ΔF
$Li_3BO_3 + \frac{3}{4}Li \rightarrow \frac{3}{4}LiBO_2 + \frac{1}{4}B + \frac{3}{2}Li_2O$	0.19	0.07	0.26
$Li_3BO_3 + Li \rightarrow 2Li_2O + \frac{1}{3}B + \frac{1}{3}B_2O_3$	0.64	0.08	0.72
$Li_3BN_2 + 3\,Li \rightarrow 2\,Li_3N + B$	1.91	0.06	1.97
$Li_3BN_2 + \frac{3}{2}\,Li \rightarrow \frac{3}{2}Li_3N + \frac{1}{2}B + \frac{1}{2}BN$	1.38	0.07	1.45

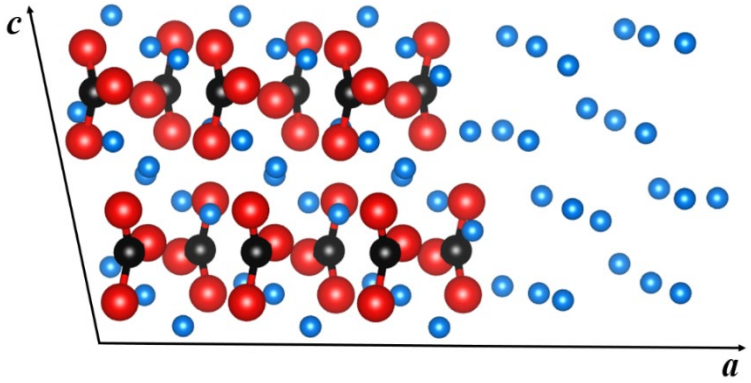

3x1x1 supercell of Li_3BO_3 and 24 metallic Li ions in [100] direction.

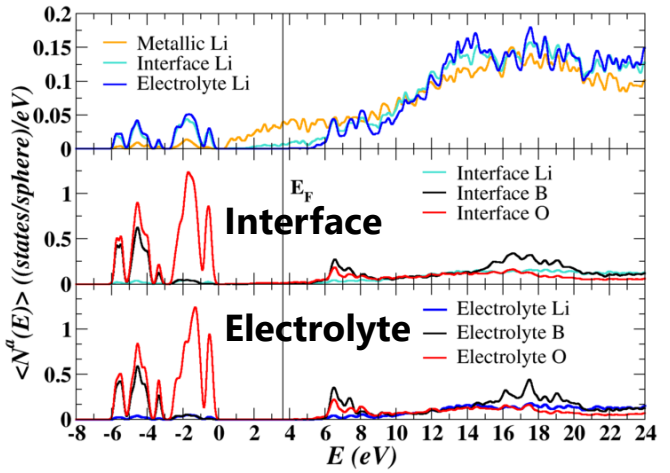

The interface energy:

$$\gamma_{ab}(\Omega, n_b) = \frac{E(\Omega, A, n_a, n_b) - n_a E_a - n_b E_b}{2A_i}$$

$$\gamma_{ab}(\Omega, n_b) = \gamma_{ab}^{\lim}(\Omega) - \sigma n_b$$

Where σ denotes the strain factor.

a -- electrolytes; b -- Li

$\sigma(Li_3BO_3/Li)$ = 19 meV/Å^2/Li

$\sigma(Li_3BN_2/Li)$ = 0.11 meV/Å^2/Li -- good compatibility

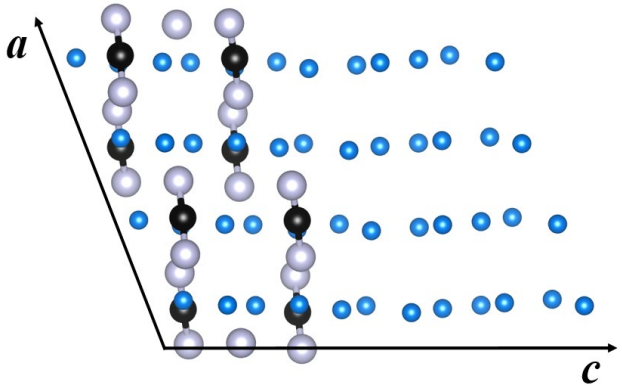

2x1x1 supercell of Li_3BN_2 and 24 metallic Li ions in [001] direction.

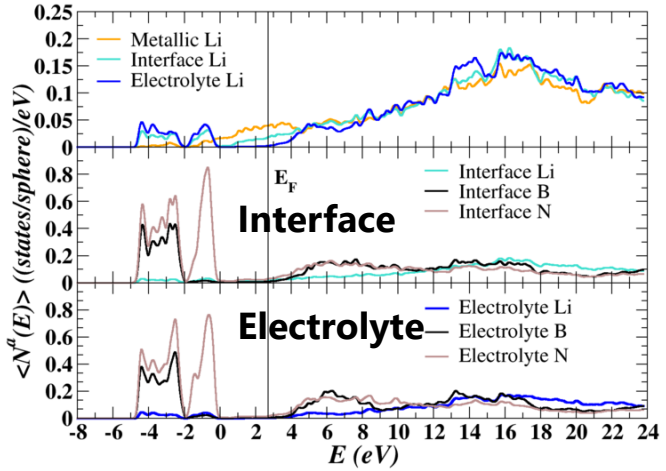

Summary

- The imaginary phonon modes near the M point of the Brillouin zone suggested the structural instability of the reported tetragonal phase of α-Li_3BN_2.
- The real α phase has an orthorhombic structure formed with twice as many formula units and very small adjustments of the fractional coordinates compared with the original analysis. Quasi-harmonic corrections further improve the comparisons with experiment.
- Both NEB and MD simulations indicate that the Li ion migration in monoclinic crystals of Li_3BO_3 and β-Li_3BN_2 most likely proceeds via vacancy mechanisms.
- To enhance the ionic conductivity, the practical methods include: 1) Varying the structural perfection to intentionally form poor-crystallinity material containing vacancy-interstitial defect pairs; 2) Substituting F for O in Li_3BO_3 and C for B in β-Li_3BN_2.
- The plausible Li_3BO_3 /Li and β-Li_3BN_2/Li interfaces are found to be physically and chemically stable.

Acknowledgements

Prof. Natalie A. W. Holzwarth
(Wake Forest University)

Dr. Zachary D. Hood
(Argonne National Laboratory)

**Computations were performed on the Wake Forest University DEAC cluster, a centrally managed resource with support provided in part by the University.

WAKE FOREST UNIVERSITY

NSF

DMR-1940324

Argonne NATIONAL LABORATORY

DE-AC02-06CH11357